PLANS AND STATUS OF HYPER-KAMIOKANDE*

Lakshmi S. Mohan

University of Silesia in Katowice, Poland
lakshmi.sandhya-mohan@us.edu.pl

Received 31 January 2026, accepted 24 February 2026, published online 22 April 2026

Hyper-Kamiokande is a next-generation water Cherenkov detector that will detect neutrinos from terrestrial and astrophysical sources in addition to probing nucleon decay. The accelerator beam neutrino program with the 258 kiloton Hyper-K as the far detector will provide high sensitivity to the unknown parameters of 3-flavour neutrino oscillation physics, especially the leptonic CP phase, $\delta_{\rm CP}$. Hyper-K will also detect atmospheric neutrinos that experience Earth matter effects and has sensitivity to neutrino mass hierarchy. The expected sensitivities to Δm^2_{32}, $\sin^2\theta_{23}$, $\delta_{\rm CP}$, and neutrino mass hierarchy from accelerator and atmospheric neutrino programs at Hyper-K are discussed here. Hyper-K is currently under construction and the data-taking is expected to commence in 2028.

DOI:10.5506/APhysPolBSupp.19.2-A11

1. Introduction

The discovery of neutrino oscillations [1] in solar and atmospheric neutrinos by the SNO [2, 3] and Super-Kamiokande (Super-K/SK) [4] experiments, respectively, established that neutrinos have a tiny but finite mass, contrary to what the Standard Model (SM) of elementary particles [5] postulated. The three active neutrino flavours ν_α ($\alpha = e, \mu, \tau$) are such that $|\nu_\alpha\rangle = \sum_{i=1}^{3} U^*_{\alpha i}|\nu_i\rangle$, where ν_i are mass eigenstates with masses m_i with $i = 1, 2, 3$. $U^*_{\alpha i}$ are the elements of a 3×3 unitary matrix called the Pontecorvo–Maki–Nakagawa–Sakata matrix $U_{\rm PMNS}$ [5, 6], parameterized by three mixing angles θ_{ij}, where $i, j = 1, 2, 3$ and one Dirac Charge Parity (CP) phase $\delta_{\rm CP}$.

The probability that a flavour ν_α oscillates to another flavour ν_β depends on θ_{ij}, $\delta_{\rm CP}$, Δm^2_{ji} (for $j > i$ where $i, j = 1, 2, 3$), and L/E, where L is the distance travelled by a neutrino of energy E. If $m_3 \gg m_2 > m_1$ ($m_2 > m_1 \gg m_3$), then neutrino masses have a normal (inverted) hierarchy.

* Presented at the XLVI International Conference of Theoretical Physics "Matter to the Deepest", Katowice, Poland, 15–19 September, 2025.

Currently, the values of θ_{23}, $|\Delta m^2_{32}|$, and $\delta_{\rm CP}$ are not known precisely. The hierarchy of neutrino masses and the octant of θ_{23} are also unknown. Several current [7–10] and future [11–13] accelerator beam and atmospheric neutrino experiments aim to measure these quantities precisely. Hyper-Kamiokande (Hyper-K/HK) [12] is one of the next-generation neutrino experiments that is currently under construction and is expected to start data-taking in 2028.

2. Hyper-Kamiokande detector

Hyper-Kamiokande is a water Cherenkov detector like its predecessor Super-K [4]. It will detect neutrinos from sources such as the Sun, the Earth's atmosphere, particle accelerator, and supernovae and will also look for nucleon decay. Hyper-K will have optically separated inner and outer detectors; the inner detector (ID) will have 20000 20-inch PMTs and 800 multi-PMTs, while the outer detector (OD) will have 3600 3-inch PMTs. The 71 m high detector with a diameter of 68 m will be filled with 258 kilotons of ultra-pure water (188 kiloton fiducial mass) with a fiducial volume ~ 8.4 times that of Super-K. The Hyper-K detector will be located in a new cavern (completed on July 31, 2025) under the peak of Mt. Nijugoyama, with 650 m of rock overburden. The schematics of the Hyper-Kamiokande detector and its location are shown in Fig. 1.

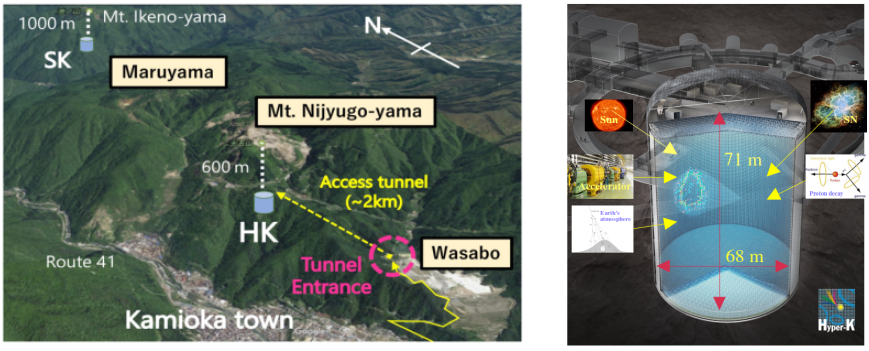

Fig. 1. Location (left) and schematic of the Hyper-K main detector (right).

3. Three-flavour neutrino oscillation physics at Hyper-K

Hyper-K will have accelerator beam and atmospheric neutrino programs to measure θ_{23}, $\Delta m^2_{32(1)}$, $\delta_{\rm CP}$, and neutrino mass hierarchy. Hyper-K sensitivities to these parameters are discussed in Sections 3.1 and 3.2, respectively.

3.1. Accelerator neutrinos at Hyper-K

The accelerator beam neutrino program will study the disappearance of ν_μ ($\bar{\nu}_\mu$) and appearance of ν_e ($\bar{\nu}_e$) in a predominantly ν_μ ($\bar{\nu}_\mu$) beam over a distance of 295 km. The (dis)appearance channels $\overset{(-)}{\nu}_\mu \to \overset{(-)}{\nu}_e$ ($\overset{(-)}{\nu}_\mu \to \overset{(-)}{\nu}_\mu$) provide the sensitivity to $\sin^2(2\theta_{13})$, the octant of θ_{23}, and the leptonic CP phase $\delta_{\rm CP}$ ($\sin^2(2\theta_{23})$ and $|\Delta m^2_{32}|$). The schematic of the accelerator beam neutrino program at Hyper-K, the oscillation probabilities at 295 km, and the impact of $\delta_{\rm CP}$ on $\overset{(-)}{\nu}_\mu \to \overset{(-)}{\nu}_e$ probabilities are shown in Fig. 2. For $\nu(\bar{\nu})$, $\delta_{\rm CP} = -\pi/2$ enhances (reduces) the probability. Since 295 km is *not very long*, the effect of $\delta_{\rm CP}$ is more dominant compared to that of mass hierarchy.

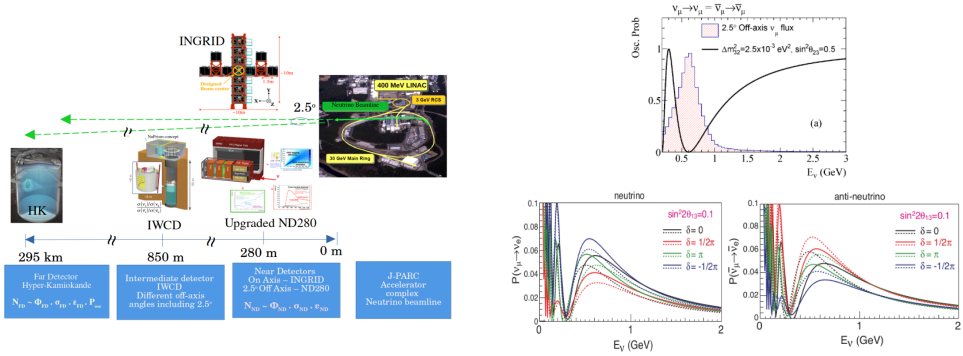

Fig. 2. Left: Schematic of the accelerator neutrino program at Hyper-K. Top right: $P_{\nu_\mu \to \nu_\mu}$ [14]; Bottom right: effect of $\delta_{\rm CP}$ on $P_{\nu_\mu \to \nu_e}$ and $P_{\bar{\nu}_\mu \to \bar{\nu}_e}$ for $L = 295$ km as a function of neutrino energy E_ν in GeV [15]. The solid (dotted) lines correspond to normal (inverted) hierarchies.

Hyper-K will have near, intermediate, and far detectors — the near detector ND280 and the far detector will be kept at an off-axis angle of 2.5° such that a narrow band neutrino beam is achieved at 0.6 GeV, where the oscillation maximum for 295 km occurs. The near detector INGRID will be on-axis and the new Intermediate Water Cherenkov Detector can be kept at different off-axis angles including 2.5°. The J-PARC neutrino beam line and the near detector ND280 used by the T2K experiment [16] have undergone several upgrades [17, 18] and will be used in the Hyper-K beam experiment. A brief description of these upgrades and new detectors for the Hyper-K beam neutrino program is given below.

Neutrino beamline: The neutrino beam for Hyper-K, where high-energy protons collide with a graphite target to produce $\pi^\pm$ that decay as $\pi^\pm \to \mu^\pm + \overset{(-)}{\nu}_\mu$ within a volume will be produced at J-PARC [17]. A predominantly ν or $\bar{\nu}$ beam is produced by adjusting the polarity of the magnetic focusing horns. With the beamline upgrade, a large number of

spills and protons (3.3×10^{14}) per spill will be achieved by reducing beam loss, instabilities, and the time between spills to 1.16 s. The upgrade of power supplies and Radio Frequency (RF) cavity systems will result in a beam power of 1.3 MW in 2028 that will enable high statistics for Hyper-K. The increase of horn current to 320 kA, aided by the upgrade of power supplies, will result in an increase in the right-sign $\nu(\bar{\nu})$ flux by 10–12% and a reduction in the wrong-sign $\bar{\nu}(\nu)$ contamination by 5–10%. The upgraded beam profile monitors will reduce the systematic uncertainties in neutrino flux measurements.

Near and Intermediate Detectors: Two near detectors currently used by the T2K experiment, INGRID and ND280, located 280 m from the production target, will provide constraints on fluxes and cross sections relevant for the sensitivities to the neutrino oscillation parameters. INGRID, the on-axis detector, will monitor the neutrino beam profile and stability. ND280, the 2.5° off-axis detector which measures the interaction cross sections and energy spectra of ν and $\bar{\nu}$ before they oscillate, has undergone significant upgrades [18]. A suite of new subdetectors — Time of Flight (TOF), a Super Fine Grained Detector (SFGD), and High Angle Time Projection Chambers (HA TPCs) [18] — allows for measuring the neutron kinematics, lowering the proton detection threshold, 3-D particle tracking and reconstruction, improving particle track acceptance, and better e/γ separation. These, along with ND280++ future upgrades, will reduce the systematic uncertainties related to flux and cross-section modelling.

Hyper-K will also have an Intermediate Water Cherenkov detector (IWCD), envisaged at a distance of 850 m from the beam production target. This detector, based on the NuPRISM [19] concept, could be moved vertically between the off-axis angles of 1.5° to 4° allowing for the probe of neutrino interactions at different flux configurations. It will provide high statistics at higher neutrino energies, while also measuring the cross sections of $\nu_e, \bar{\nu}_e, \nu_\mu$, and $\bar{\nu}_\mu$; the cross-section ratios $\frac{\sigma_{\nu_e}}{\sigma_{\nu_\mu}}$, $\frac{\sigma_{\bar{\nu}_e}}{\sigma_{\bar{\nu}_\mu}}$, and their double ratios. Thus, IWCD, along with the upgraded ND280 detector, will reduce the systematic uncertainties that affect the sensitivity to CP violation (CPV) at Hyper-K.

Far detector Hyper-K: The far detector of the Hyper-Kamiokande LBL program will be located 295 km from the beam production target at an off-axis angle of 2.5°. Hyper-K ID will have 20000, 50 cm box and line type PMTs which have better photon detection efficiencies, charge, and timing resolutions compared to the PMTs used in Super-K. Though Hyper-K will only have half the photo coverage of Super-K, a performance comparable to Super-K can be achieved with these new PMTs.

3.1.1. Sensitivities to 3-flavour neutrino oscillation parameters

The expected sensitivities to different 3-flavour neutrino oscillation parameters of interest are discussed here. The studies [12] assume 10 years of statistics taken with 2.7×10^{21} proton on target (POT) per calendar year (6.75×10^{21} POT in ν and 20.25×10^{21} POT in $\bar{\nu}$, corresponding to a ratio of 1:3). The central values of oscillation parameters used are shown in Table. 1. Different cases of models and systematic uncertainties are also considered for the study — (a) statistical uncertainty only, (b) T2K models and parametrization of uncertainties on neutrino flux, neutrino–nucleus interaction cross section, and detector response (same as in [20]), and (c) improved systematic uncertainties (with statistical errors from the near detector dominating over systematic errors) — assuming errors constrained by ND280 and far detector systematics scaled by $1/\sqrt{N}$, where $N = 7.5$ (assumption of similar far detector data taking between T2K and Hyper-K), from upgraded ND280 and IWCD.

Table 1. Central values of oscillation parameters used in the sensitivity study.

$\sin^2\theta_{12}$	$\Delta m^2{}_{21}$ [eV^2]	$\sin^2\theta_{23}$	$\Delta m^2{}_{32}$ [eV^2]	$\sin^2\theta_{13}$	$\delta_{\rm CP}$ [radians]	Mass hierarchy
0.307	7.53×10^{-5}	0.528	2.501×10^{-3}	0.0218	-1.601	normal

Sensitivities when the true mass hierarchy is known as normal (NH) are discussed here. Sensitivity to CP violation as a function of time is shown in Fig. 3. The solid, dashed, and dotted lines indicate the different systematic error scenarios considered. The black (red) band in the left panel of Fig. 3

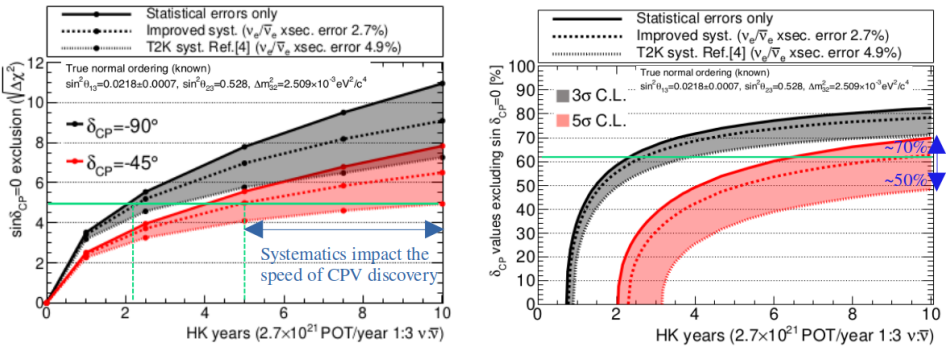

Fig. 3. Left: Sensitivity to CP violation as a function of exposure time in years. Right: Percentage of true $\delta_{\rm CP}$ values for which CP conservation can be excluded at 3 and 5σs as a function of exposure time in years. The figures are from [12].

corresponds to $\sqrt{\Delta\chi^2}$ to exclude $\sin\delta_{\rm CP} = 0$ for true $\delta_{\rm CP} = -90\ (-45)^\circ$. If $\delta_{\rm CP}^{\rm true} = -90^\circ$, a 5σ discovery of CPV is possible in less than 3 years. For $\delta_{\rm CP}^{\rm true} = -45^\circ$, a 5σ discovery of CPV will only be possible in less than 6 years even with improved systematic uncertainties. Thus, the systematics impact the speed of CPV discovery. For a given systematic uncertainty scenario, the CPV discovery potential is always larger for $\delta_{\rm CP} = -90^\circ$. The right panel of Fig. 3 corresponds to the percentage of true values of $\delta_{\rm CP}$ for which CP conservation can be excluded at 3 $(5)\sigma$ — black (red) bands. With improved systematics, CPV discovery is possible at 5σ for 60% of true $\delta_{\rm CP}$ values with 10 years of exposure. The figure also shows that CPV sensitivity is the most degraded by the uncertainty on $\sigma(\nu_e)/\sigma(\bar{\nu}_e)$ cross-section ratio.

Precision on $\delta_{\rm CP}$ with true mass ordering known as normal: The precision on $\delta_{\rm CP}$ for different true $\delta_{\rm CP}$ values is shown in Fig. 4. The factors affecting the achievable precision are the true values of $\delta_{\rm CP}$ and the systematic uncertainties. The precision improves with an increase in exposure time and is always better for a true CP conserving value (*i.e.* $\delta_{\rm CP} = 0^\circ, \pm 180^\circ$) than for a true CP violating value ($\delta_{\rm CP} = \pm 90^\circ$). At a given $\delta_{\rm CP}^{\rm true}$ value, the precision becomes better with the improvement in the systematic error model as the error on $\nu_e/\bar{\nu}_e$ cross-section error reduces.

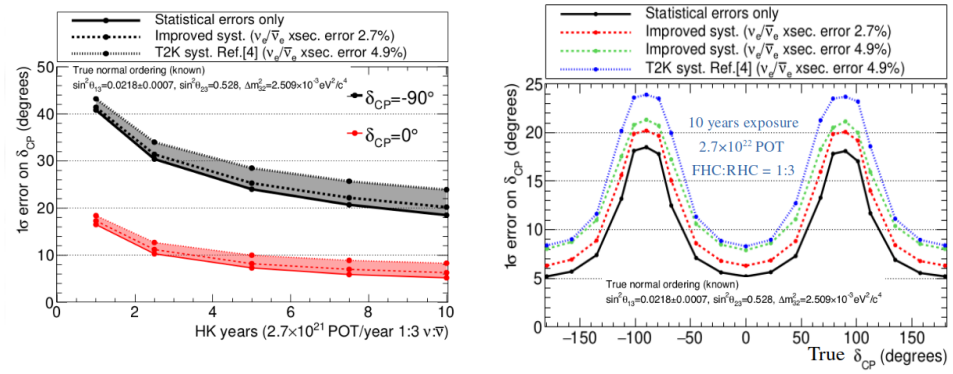

Fig. 4. Left: 1σ error on $\delta_{\rm CP}$ as a function of exposure time in years for $\delta_{\rm CP}^{\rm true} = -\pi/2$ and 0; right: as a function of $\delta_{\rm CP}^{\rm true}$ for 10 years of exposure time. The results are shown for different uncertainties on $\sigma(\nu_e)/\sigma(\bar{\nu}_e)$. The figures are from [12].

The achievable resolution on $\delta_{\rm CP}$ can be evaluated by considering the derivative of appearance probability $P_{\nu_\mu \to \nu_e}$ with respect to $\delta_{\rm CP}$ [12]. For $\delta_{\rm CP}^{\rm true} = 0, \pm\pi$, $\sin\delta_{\rm CP} = 0$, but its derivative $\cos\delta_{\rm CP}$ is maximal. Thus, the precision for $\delta_{\rm CP}^{\rm true}$ around CP conserving values is a measure of the difference between ν_e and $\bar{\nu}_e$ events. Here, the $\sigma\nu_e/\sigma_{\bar{\nu}_e}$ cross-section ratio has a significant impact on the resolution. For $\delta_{\rm CP}^{\rm true} \approx \pm 90^\circ$ (maximal CP violating values), $\cos\delta_{\rm CP} = 0$, but its derivative $-\sin\delta_{\rm CP}$ is maximal. Here, the

$\cos\delta_{\rm CP}$-induced shape effects on the energy spectra of ν_e and $\bar{\nu}_e$ dominate, thus making the systematic effects related to neutrino reconstructed energy more relevant. The uncertainties relevant in each case will be constrained experimentally with data from the ND280++ upgrade and IWCD.

Constraints on θ_{23} and $|\Delta m^2_{32}|$: The ability to exclude the wrong octant of θ_{23} for different systematic error cases is shown in Fig. 5. The left panel shows the wrong exclusion sensitivity as a function of $\sin^2\theta^{\rm true}_{23}$ for an exposure time of 10 years. The right panel shows the ability to exclude the wrong octant at 3σ as a function of exposure time in years for different $\sin^2\theta^{\rm true}_{23}$. The wrong octant exclusion is the worst for $\sin^2\theta^{\rm true}_{23} = 0.5$ (maximal mixing). For a given $\sin^2\theta^{\rm true}_{23}$ value, this sensitivity increases with improvement in the systematic uncertainties.

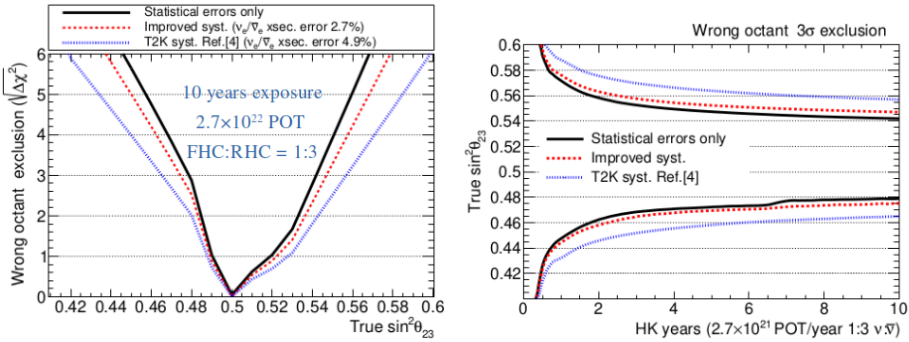

Fig. 5. Left: Sensitivity to reject the wrong octant of θ_{23} after 10 years exposure time. Right: CP violation as a function of exposure time in years to reject the wrong octant at 3σ as a function of time for different true values of $\sin^2\theta_{23}$. The figures are from [12].

The precision on $\sin^2\theta_{23}$ and Δm^2_{32} achievable with different systematic error scenarios is shown in Fig. 6. The left (right) panel shows the 1σ error on $\sin^2\theta_{23}$ (Δm^2_{32}) as a function of exposure time in years, for $\sin^2\theta_{23} = 0.528$. The middle panel shows the precision on $\sin^2\theta_{23}$ after 10 years of exposure

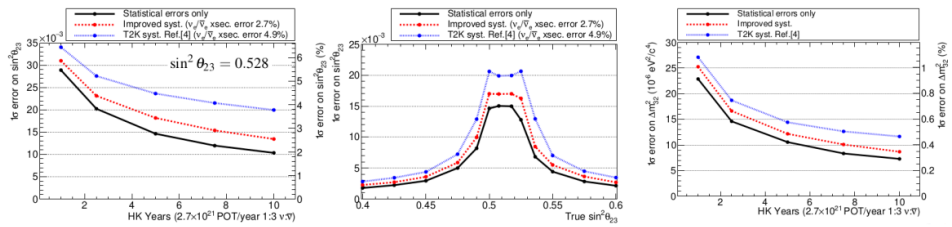

Fig. 6. Precision on $\sin^2\theta_{23}$ (Δm^2_{32}) from the Hyper-K beam neutrino program, see the text. The figures are from [12].

for different true values of $\sin^2\theta_{23}$. An ultimate resolution of 0.2%–0.4% (0.4%) can be achieved for $\sin^2\theta_{23}$ (Δm^2_{32}), depending on (irrespective of) the true values of oscillation parameters.

3.2. Atmospheric neutrinos at Hyper-K

The sensitivities discussed in Section 3.1.1 assumed that the true hierarchy was known to be normal. However, we still do not know the true hierarchy of neutrinos, which means that the sensitivity to CPV is degraded in regions where δ_{CP} and mass hierarchy are degenerate as shown in Fig. 7. An independent determination of mass hierarchy with atmospheric neutrinos can lift this degeneracy.

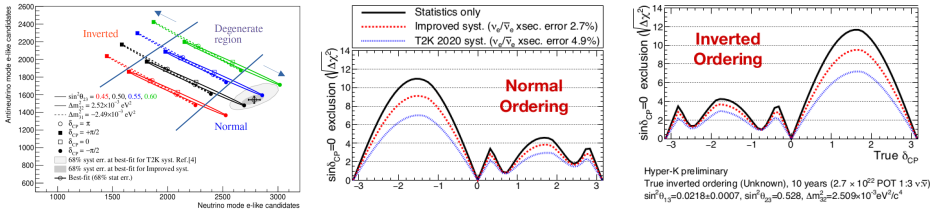

Fig. 7. Left: Degeneracy of δ_{CP} and mass hierarchy for 295 km [12]. Middle and right: Degradation of CPV sensitivity in the degenerate regions when the true mass ordering is not known [21].

Neutrinos propagating inside the Earth undergo coherent forward elastic scattering with the electrons and nucleons in it, resulting in a net potential that modifies neutrino mixing and time evolution of the flavour states. The effective charge current potential $A_{CC} = 7.63\times10^{-5}\rho E$ (eV^2) (where ρ is the matter density in (g/cm^3) and E is the neutrino energy in GeV) is positive (negative) for ν ($\bar{\nu}$). *Matter resonance* occurs for ν ($\bar{\nu}$) if neutrino mass hierarchy is normal (inverted) as illustrated in Fig. 8. True mass hierarchy can be determined independent of δ_{CP} by the observation of resonance in atmospheric neutrinos ($\sim$ 80 atmospheric neutrino events/day in Hyper-K) that travel varying ρ through the Earth. The wide range of L/E spanned by atmospheric neutrinos is very advantageous here. The effect of different oscillation parameters and hierarchies on the ratio of oscillated to unoscillated ν_e flux for the zenith angle $\cos\theta_\nu = -0.8$ is also shown in Fig. 8.

The sensitivities to mass hierarchy and the ability to reject wrong octant with atmospheric neutrinos alone and in combination with accelerator beam neutrino data are shown in Fig. 9. The sensitivity to hierarchy increases with the increase in $\sin^2\theta_{23}$. For $\sin^2\theta^{true}_{23} = 0.5$, $\sim 3\sigma$ rejection of wrong hierarchy is possible with 10 years of atmospheric neutrino data alone; this increases to about $\sim 5\sigma$ when beam neutrino data is also added. With

10 years of atmospheric neutrino data alone, a $\sim 3\sigma$ rejection of the wrong octant is possible if $|\theta_{23} - 45°| > 4°$. Combining with beam data, 3σ rejection of wrong octant is possible if $|\theta_{23}| > 2.3°$.

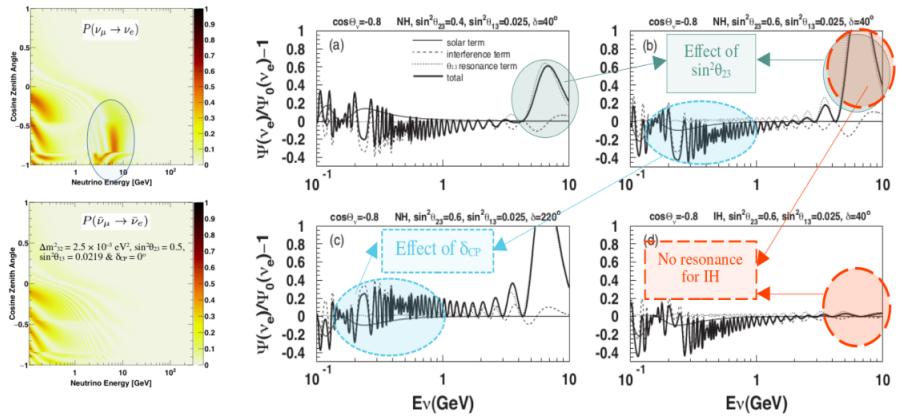

Fig. 8. Left top: $\nu_\mu \to \nu_e$ (left bottom) $\bar{\nu}_\mu \to \bar{\nu}_e$ in the presence of Earth matter, for true normal hierarchy [10]. Matter resonance (highlighted with the blue ellipse) occurs for $\nu(\bar{\nu})$ when the true hierarchy is normal (inverted). The middle and right panels show the effect of different oscillation parameters on the ratio of the oscillated to unoscillated ν_e flux for $\cos\theta_\nu = -0.8$ [22]. For a given hierarchy (NH) and other oscillation parameters fixed at a particular value, the size of the resonance is enhanced for larger $\sin^2\theta_{23}$ at higher energies; the effect of δ_{CP} can be seen at sub-GeV energies, whereas there will be no resonance if the hierarchy is inverted.

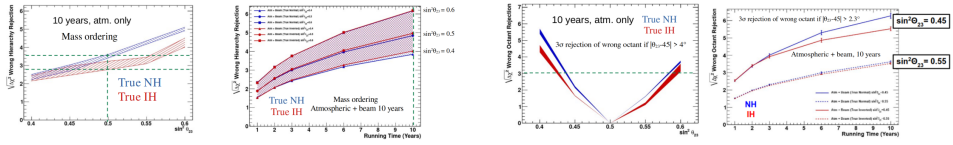

Fig. 9. Sensitivity to the reject wrong (left) hierarchy (right) octant with atmospheric neutrinos alone and beam+atmospheric neutrinos in Hyper-K. The figures are from [22].

4. Conclusions

Hyper-Kamiokande (Hyper-K) will detect neutrinos from several sources including particle accelerators, Earth's atmosphere, the Sun, and supernovae in addition to probing nucleon decay. As discussed in these proceedings, the accelerator neutrino program at Hyper-K will have unprecedented sensitivities to the possible determination of CP violation (or its exclusion) in the

leptonic sector, the rejection of the wrong octant of θ_{23}, and improved precision on $\sin^2\theta_{23}$ and $|\Delta m^2_{32}|$. Combined with the atmospheric neutrino program, the degeneracies in the determination of $\delta_{\rm CP}$ and neutrino mass hierarchy can be lifted, further improving the sensitivities to the neutrino oscillation parameters of interest. Hyper-Kamiokande, which is expected to commence data-taking in 2028, will thus provide competitive neutrino oscillation programs that will advance the field of neutrino physics.

REFERENCES

[1] «Neutrino Oscillations», https://www.nobelprize.org/prizes/physics/2015/press-release/

[2] SNO Collaboration (Q.R. Ahmad *et al.*), *Phys. Rev. Lett.* **87**, 071301 (2001).

[3] SNO Collaboration (S.N. Ahmed *et al.*), *Phys. Rev. Lett.* **92**, 181301 (2004).

[4] Super-Kamiokande Collaboration (Y. Fukuda *et al.*), *Phys. Rev. Lett.* **81**, 1562 (1998).

[5] Particle Data Group (S. Navas *et al.*), *Phys. Rev. D* **110**, 030001 (2024).

[6] C. Giunti, C.W. Kim, «Fundamentals of Neutrino Physics and Astrophysics», *Oxford University Press*, 2007.

[7] T2K Collaboration (K. Abe *et al.*), *Nature* **580**, 339 (2020); *Publisher correction ibid.* **583**, E16 (2020).

[8] NOvA Collaboration (M.A. Acero *et al.*), *Phys. Rev. D* **110**, 012005 (2024).

[9] IceCube Collaboration (R. Abbasi *et al.*), *Phys. Rev. D* **108**, 012014 (2023).

[10] Super-Kamiokande Collaboration (T. Wester *et al.*), *Phys. Rev. D* **109**, 072014 (2024).

[11] Hyper-Kamiokande Proto-Collaboration (K. Abe *et al.*), *Prog. Theor. Exp. Phys.* **2015**, 053C02 (2015).

[12] Hyper-Kamiokande Collaboration, arXiv:2505.15019 [hep-ex].

[13] DUNE Collaboration (B. Abi *et al.*), *Eur. Phys. J. C* **80**, 978 (2020).

[14] T2K Collaboration (D. Karlen), *Universe* **5**, 21 (2019).

[15] K. Abe *et al.*, arXiv:1109.3262 [hep-ex].

[16] K. Abe *et al.*, *Nucl. Instrum. Methods Phys. Res. A* **659**, 106 (2011).

[17] M. Friend, *J. Phys.: Conf. Ser.* **888**, 012042 (2017).

[18] K. Abe *et al.*, arXiv:1901.03750 [physics.ins-det].

[19] S. Bhadra *et al.*, arXiv:1412.3086 [physics.ins-det].

[20] T2K Collaboration (K. Abe *et al.*), *Eur. Phys. J. C* **83**, 782 (2023).

[21] Hyper-Kamiokande Collaboration (C. Dalmazzone), *PoS* **(EPS-HEP2025)**, 156 (2025).

[22] K. Abe *et al.*, arXiv:1805.04163 [physics.ins-det].